ANTICANCER RESEARCH *41*: 2963-2977 (2021)
doi:10.21873/anticanres.15078

Pemetrexed Disodium Heptahydrate Induces Apoptosis and Cell-cycle Arrest in Non-small-cell Lung Cancer Carrying an EGFR Exon 19 Deletion

MD MOHIUDDIN and KAZUO KASAHARA

Department of Respiratory Medicine, Kanazawa University, Ishikawa, Japan

Abstract. *Background/Aim: Non-small-cell lung cancer (NSCLC) remains a significant cause of death despite the recent introduction of several improved therapeutics. Pemetrexed disodium heptahydrate (pemetrexed) is currently available in combination with a platinum derivative for patients with advanced non-squamous NSCLC for first-line treatment, and as a single agent for second-line treatment. However, the mechanisms underlying its anticancer activities are still not well understood. In this study, we evaluated the growth inhibitory effects of pemetrexed on PC9 (EGFR exon 19 deletion) cells and elucidated the underlying molecular mechanisms. Materials and Methods: PC9 cells were treated with pemetrexed and then assessed for the cell viability, morphological and nuclear changes, antigenic alterations, SA-β-gal staining, and changes in protein expression. Results: Pemetrexed reduced the cell viability of PC9 cells and initiated cell morphological changes in a concentration-dependent manner. Pemetrexed significantly induced G_1 phase arrest in a dose-dependent manner. The results demonstrated that pemetrexed induced apoptosis in PC9 cells, a change coupled with an increase in reactive oxygen species and a decrease in mitochondrial membrane potential. Pemetrexed decreased Bcl-2 expression, while Bax expression was increased, and cytochrome c was released. Furthermore, the expression of extrinsic pathway proteins, e.g. Fas/FasL, DR4/TRAIL, and Fas-associated protein with death domain, was increased by pemetrexed, which then activated caspase-8, caspase-9, and caspase-3 and induced poly (ADP-ribose) polymerase proteolysis. Conclusion: This study revealed the mechanisms by which pemetrexed works an anticancer drug in the treatment of NSCLC.*

Correspondence to: Md Mohiuddin, Department of Respiratory Medicine, Graduate School of Medical Sciences, Kanazawa University, 13-1 Takaramachi, Kanazawa, Ishikawa 920-8641, Japan. Tel: +81 7022501723, e-mail: mohiuddin@med.kanazawa-u.ac.jp

Key Words: Pemetrexed, PC9 cells, apoptosis, caspases, cell-cycle arrest.

Non-small-cell lung cancer (NSCLC) is the world's leading cause of disease-related deaths, with an estimated 154,000 deaths in the United States in 2018 (1). Pemetrexed is a multi-focused anti-folate agent used to treat non-squamous NSCLC and malignant pleural mesothelioma (2). For advanced NSCLC and locally advanced NSCLC treatment, pemetrexed is currently combined with cisplatin or carboplatin as a first-line treatment (3). In addition, pemetrexed is also used as a single drug in second-line therapy for maintenance therapy after platinum chemotherapy (3, 4).

Apoptosis is a form of programmed cell death (PCD) that can happen in multicellular organisms (5). Apoptosis can be initiated through two important pathways: the extrinsic pathway (death receptor) and the intrinsic pathway (mitochondrial) (6). Programmed cell death occurs due to various types of stress. Reactive oxygen species (ROS) production (7) is a key stressor triggering DNA damage (8). The transducer kinases Chk1 and Chk2, which are activated by ataxia-telangiectasia mutated (ATM) and ataxia–telangiectasia and Rad3-related (ATR), respectively, regulate the proteins involved in the DNA damage response (DDR), DNA repair, and arrest of cell-cycle progression (9).

In cancer cells, chemotherapy or radiotherapy can increase ROS production, which activates the death signal cascade (10). The proapoptotic proteins Bak and Bax activate the intrinsic apoptosis pathway (11) by decreasing the mitochondrial membrane potential (MMP). The loss of the MMP causes the release of cytochrome *c* from the mitochondria, which leads to caspase cascade activation (12). Furthermore, following DNA damage, p53 activates the extrinsic apoptotic pathway by up-regulating death receptors (TNFR1, Fas, DR3, DR4, *etc.*) and ligands (FasL, TRAIL, etc.) (13). After the stimulation of a death receptor, caspase-8 is activated, which recruits the adapter molecule Fas-associated protein with death domain (FADD) and induces further processing of procaspase-8 (14). Caspase-8 induces the depolarization of the MMP by Bid cleaving into truncated Bid (tBid), thereby initiating the mitochondrial apoptosis pathway (15) and leading to cytochrome *c* release from mitochondria

into the cytosol. Released cytochrome *c* binds to Apaf-1 to form a heptameric apoptosome, which activates the caspase family (16). Finally, poly (ADP-ribose) polymerase (PARP) metabolism induced by DNA damage contributes to DNA repair and participates in cell-cycle arrest, cell death, and cell survival signaling mechanisms (17).

Following DNA damage, the cyclin-dependent kinase inhibitors p21 and p27 bind to cyclin-Cdk complexes to impede their catalytic activity and induce cell-cycle arrest (18). Cyclin D-Cdk4/6 complexes [explicitly targeted by transforming growth factor-β (TGF-β) signal] cause G_1 phase arrest *via* the induction of $p15^{INK4B}$, a negative regulator of Cdk4/6 (19-21). However, resistance to chemotherapy is evident after lung cancer therapy (22). It is therefore necessary to test new anticancer drugs with high therapeutic efficacy and lung cancer selectivity. Furthermore, senescence appears to play a central role in anticancer drugs initiated by various anticancer medications and ionizing radiation (23-25).

In this study, we aimed to elucidate the mechanism underlying the anticancer effects of pemetrexed on PC9 cells. We herein report the impact of pemetrexed on growth inhibition in PC9 cells.

Materials and methods

Cell line and cell culture. The EGFR exon 19 deletion (Ex19Del) mutated human NSCLC cell line PC9 derived from a patient with previously untreated adenocarcinoma was kindly donated by Professor K. Hayata (Tokyo Medical College, Tokyo, Japan) (26). PC9 cells were cultured in RPMI 1640 medium (Invitrogen, Grand Island, NY, USA) containing 10% fetal bovine serum (FBS; Invitrogen) and maintained at 37˚C in a humidified atmosphere containing 5% CO_2.

Drug preparation. Pemetrexed disodium heptahydrate [C20H19N5Na206•7H2O] was obtained from FUJIFILM Wako Pure Chemical Corporation (Osaka, Japan). This drug was dissolved in DMSO for *in vitro* experiments.

Cell proliferation assay. The water-soluble tetrazolium salt (WST-1) assay (Cell Proliferation Reagent WST-1; Roche, Tokyo, Japan) was used to evaluate the cytotoxicity of different pemetrexed concentrations. A 100-μl volume of a growing cell suspension was seeded into each well (4×10^3 cells/well) of a 96-well microtiter plate, and 100 μl of a solution of pemetrexed at various concentrations was added to each well. After incubation for 72 h at 37˚C in a 5% carbon dioxide atmosphere, 10 μl of WST-1 solution was added to each well, and the plates were incubated at 37˚C for a further 4 h. Using a microplate enzyme-linked immunosorbent assay reader (Multiskan FC; Thermo Scientific, Tokyo, Japan), these samples' absorbance was measured at 450 nm.

Giemsa and DAPI staining. For 72 h, PC9 cells were treated in 12-well plates with various concentrations of pemetrexed. DAPI (Invitrogen) was used to stain cells fixed in 4% paraformaldehyde in phosphate-buffered solution (FUJIFILM Wako Pure Chemical Corporation) and permeabilized with 0.1% Triton X-100 (Sigma-Aldrich, Tokyo, Japan). The morphology of cell nuclei was observed using a BZ-X710 All-in-One Fluorescence Microscope (Keyence, Osaka, Japan). Giemsa staining (Merck KGaA, Darmstadt, Germany) was performed with methanol-fixed cells, and morphological changes were evaluated under a light microscope.

Intracellular ROS assay. The intracellular ROS level was detected using the Reactive Oxygen Species Detection Assay Kit (ab186029; Abcam, Tokyo, Japan). In brief, after treatment with various concentrations of pemetrexed for 72 h, cells were harvested for staining with a working solution of deep red ROS dye. Subsequently, the cells were incubated at 37˚C for 60 min before the flow cytometry (FCM) analysis.

Terminal deoxynucleotidyl transferase dUTP nick-end labeling (TUNEL) assay. The PC9 cells were treated with different concentrations of pemetrexed for 72 h. According to the manufacturer's guidelines, to measure DNA fragmentation in apoptotic cells, we used the in situ Direct DNA Fragmentation (TUNEL) Assay Kit (ab66108; Abcam). In brief, cells were fixed with 1% paraformaldehyde in PBS and placed on ice for 15 min. Subsequently, the samples were treated with a staining solution and incubated at 37˚C for 60 min. After adding the rinse buffer, cells were resuspended in propidium iodide/RNase A solution and incubated for 30 min at room temperature and examined by flow cytometry.

MMP assay. Following pemetrexed treatment, intracellular MMP changes were evaluated using a JC-10 Mitochondrial Membrane Potential Assay Kit (ab112133; Abcam). In brief, cells were trypsinized, washed with PBS, and incubated with 1X JC-10 dye-loading solution at room temperature for 30 min. Using BD FACSCantoTM II (BD Biosciences, San Jose, CA, USA), the cell fluorescence was measured.

Annexin V-FITC/PI apoptosis assay. Using an Annexin V-FITC/PI apoptosis detection kit (BioLegend, San Diego, CA, USA), cell apoptosis was detected. In brief, after treatment with various concentrations of pemetrexed for 72 h, cells were stained with Annexin V-FITC and PI. They were then analyzed by FCM (FACSCantoTM II), and their fluorescence intensity was detected. Data were analyzed using the FlowJo software program, version 10.2 (FLOWJO, LLC, Ashland, OR).

Western blotting. For 72 h, PC9 cells were treated with different concentrations of pemetrexed. Whole protein lysates were isolated using the M-PER mammalian protein extraction reagent (Thermo Scientific), included a phosphatase inhibitor cocktail and a protease inhibitor cocktail (Sigma-Aldrich). Using a Cytosol and Mitochondrial Protein Extraction Kit (ab65320; Abcam), mitochondrial and cytosolic proteins were separated. Protein concentrations were assessed using the BCA protein assay reagent (Thermo Scientific). Total cellular protein (40 μg) was separated by sodium dodecyl sulfate-polyacrylamide gel electrophoresis (SDS-PAGE) and transferred to polyvinylidene fluoride membranes (Bio-Rad Laboratories, Hercules, CA, USA). Milk-blocked blots were incubated at 4˚C overnight with primary antibodies of Bcl-2 (Cell Signaling Technology, Beverly, MA, USA), TRAIL (Cell Signaling Technology), Cyclin D1 (BioLegend), Cdk4 (Cell Signaling Technology), DR4 (Cell Signaling Technology), FADD (Cell Signaling Technology), PARP (Cell Signaling Technology), Cleaved caspase-3 (Asp 175) (Cell Signaling Technology), Cleaved caspase-6 (Asp 162) (Cell Signaling Technology), Cleaved caspase-7 (Asp 198) (Cell

Signaling Technology), Caspase-9 (Cell Signaling Technology), Caspase-8 (Cell Signaling Technology), Bid (Cell Signaling Technology), Apaf-1 (Cell Signaling Technology), Cytochrome *c* (Cell Signaling Technology), Bax (Cell Signaling Technology), Fas (Cell Signaling Technology), FasL (Cell Signaling Technology), TGF-β (Cell Signaling Technology), p-ATR (Ser 428) (Cell Signaling Technology), p-Smad2 (Ser 465/467)/Smad3 (Ser 423/425) (Cell Signaling Technology), $p15^{INK4B}$ (Cell Signaling Technology), p-Chk1 (Ser 345) (Cell Signaling Technology), phospho-p53 (Ser 15) (Cell Signaling Technology), phospho-p53 (Ser 46) (Cell Signaling Technology), and γ-H2AX (Phospho S140; Abcam) and then with appropriate horseradish peroxidase-conjugated secondary antibodies (Cell Signaling Technology). Proteins of interest were revealed using SuperSignal West Pico PLUS Chemiluminescent Substrate (Thermo Fisher Scientific, Rockford, IL, USA) and viewed using the Invitrogen iBright FL1000 Imaging System (Thermo Fisher Scientific).

Cell-cycle analysis. The cells were treated with different concentrations of pemetrexed for 72 h. A cell-cycle analysis was performed following the Propidium Iodide Cell-Cycle Staining Protocol (BioLegend). DNA content was determined with a FACSCantoTM II. Data were analyzed using the FCS Express 7 Flow software program (De Novo Software, Pasadena, CA, USA).

Senescence-associated β-galactosidase (SA-β-gal) staining. Cells were treated with different concentrations of pemetrexed for 72 h. For SA-β-gal staining, we used a Senescence-β-gal Staining Kit (Cell Signaling Technology) according to the manufacturer's instructions.

Statistical analysis. Using the GraphPad PRISM 7.0 software program (GraphPad Software Inc., San Diego, CA, USA), graphs were created. Results are presented as the mean±standard deviation (SD) of three independent experiments evaluated using a one-way ANOVA followed by Dunnett's multiple comparison test. If $*p<0.05$, $**p<0.01$ and $***p<0.001$, then the mean was considered significantly different.

Results

Cytotoxic effects of pemetrexed in PC9 cells. PC9 cells were treated with 2 concentrations of pemetrexed (50 and 100 nM) for 72 h, and the WST-1 assay was used to assess the cell viability. The viability of PC9 cells decreased in a dose-dependent manner after pemetrexed treatment (Figure 1A). Cells were stained with Giemsa and DAPI to investigate the morphological changes induced by pemetrexed. Cells undergoing pemetrexed treatment showed morphological signs of oncosis, such as cell swelling (green arrows), membrane blebbing (red arrows), and nuclear swelling (black arrows) (Figure 1B). DAPI staining indicated nuclear swelling (yellow arrows) of PC9 cells in response to pemetrexed treatment (Figure 1C).

Pemetrexed increased ROS levels and enhanced DNA fragmentation in PC9 cells. ROS generation is an indicator of cell apoptosis. The intracellular ROS level was measured by FCM. Compared to vehicle-only cells, pemetrexed increased the ROS level in a dose-dependent manner (Figure 2). These changes were accompanied by DNA fragmentation, a key marker of apoptosis (Figure 3A and B).

Pemetrexed regulated the DNA damage signaling pathway. After the pemetrexed treatment of PC9 cells, we evaluated the expression of proteins associated with DNA damage. ATM and ATR play key roles in major cell processes, including proliferation and genomic surveillance (27). Activation *via* phosphorylation of these proteins (ATM and ATR) promotes cell-cycle arrest and apoptosis through the consequent phosphorylation of downstream factors (p53, H2AX, Chk2, Chk1, *etc*.) (28, 29). Chk1 and Chk2 are serine-threonine kinases activated by phosphorylation at Ser 345 or Thr 68 by ATR or ATM kinases, respectively (27). As presented in Figure 3C, the expression of phospho-p53 (Ser 15), phospho-p53 (ser 46), γ-H2AX (Phospho S140), p-ATR (Ser 428) and p-Chk1 (Ser 345) was increased after pemetrexed treatment in a dose-dependent manner. These results indicate that pemetrexed plays an essential role in response to DNA damage mediated by ATR-Chk1 signaling in the activation of p53 during pemetrexed treatment of PC9 cells.

Pemetrexed decreased the MMP in PC9 cells. ROS alter the MMP and structure (30). We used the fluorescent cationic dye JC-10 to check the potential of mitochondrial membrane depolarization. In non-apoptotic cells, the negative charge generated by the mitochondrial membrane ideal potential caused the accumulation of JC-10 in the mitochondria and the formation of "J aggregates" that emit red fluorescence. Conversely, the mitochondrial membrane can be destroyed in apoptotic cells, leaving green monomer fluorescence of JC-10 in the cytoplasm (31). In pemetrexed-treated PC9 cells, JC-10 monomer cells dominated in the lower MMP area (right lower quadrant 3), indicating that pemetrexed impaired the mitochondrial integrity through concentration-dependent MMP loss (Figure 4).

Pemetrexed induced apoptosis and regulated the apoptosis signaling pathways in PC9 cells. To prove that the cell death caused by pemetrexed was indeed apoptosis, we conducted Annexin V and PI staining for an FCM analysis. As shown (Figure 5A), after 72 h of exposure to pemetrexed, the proportion of late apoptotic cells (upper right quadrant 2, Annexin V/PI-positive) increased from 4.48% to 22.1%. FCM showed that the pemetrexed-induced apoptosis was concentration-dependent (Figure 5B).

After 72 h of treatment of PC9 cells with different pemetrexed concentrations, Western blotting was performed to assess the expression of key proteins of the extrinsic and intrinsic apoptotic pathways, including Bax, Bcl-2, tBid, cleaved caspase-6 (Asp 162), cleaved caspase-3 (Asp 175), cleaved caspase-8, Fas, cleaved caspase-7 (Asp 198), cleaved

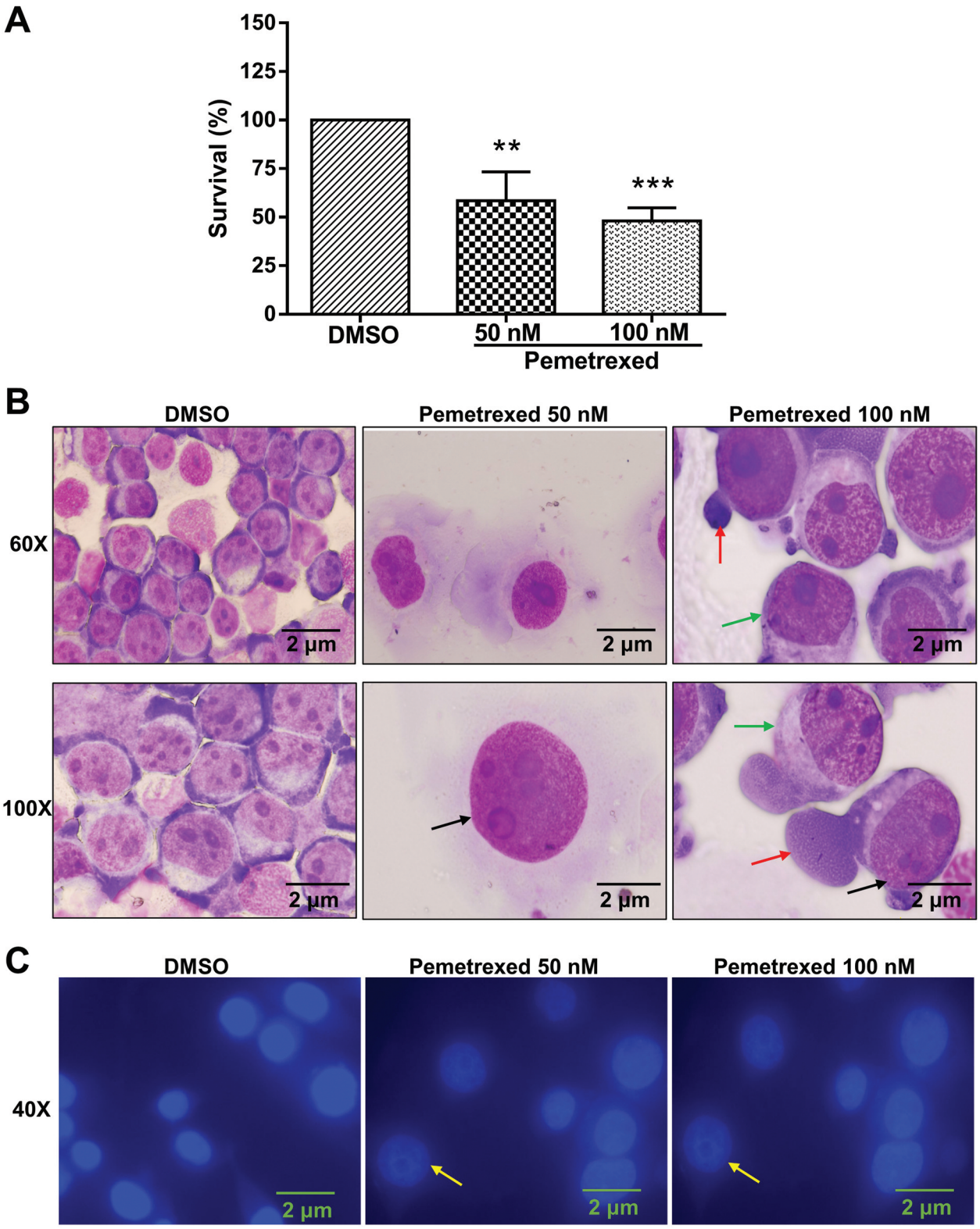

Figure 1. *Impact of pemetrexed on the viability and morphology of PC9 cells. (A) The WST-1 cell proliferation assay was used to evaluate cell viability of PC9 cells treated with different concentrations of pemetrexed for 72 h; n=3, mean±SD; Significance was determined by a one-way ANOVA followed by Dunnett's multiple comparison test: **p<0.01 and ***p<0.001 compared with the DMSO group. (B) DAPI and (C) Giemsa staining of PC9 cells treated under different concentrations of pemetrexed for 72 h.*

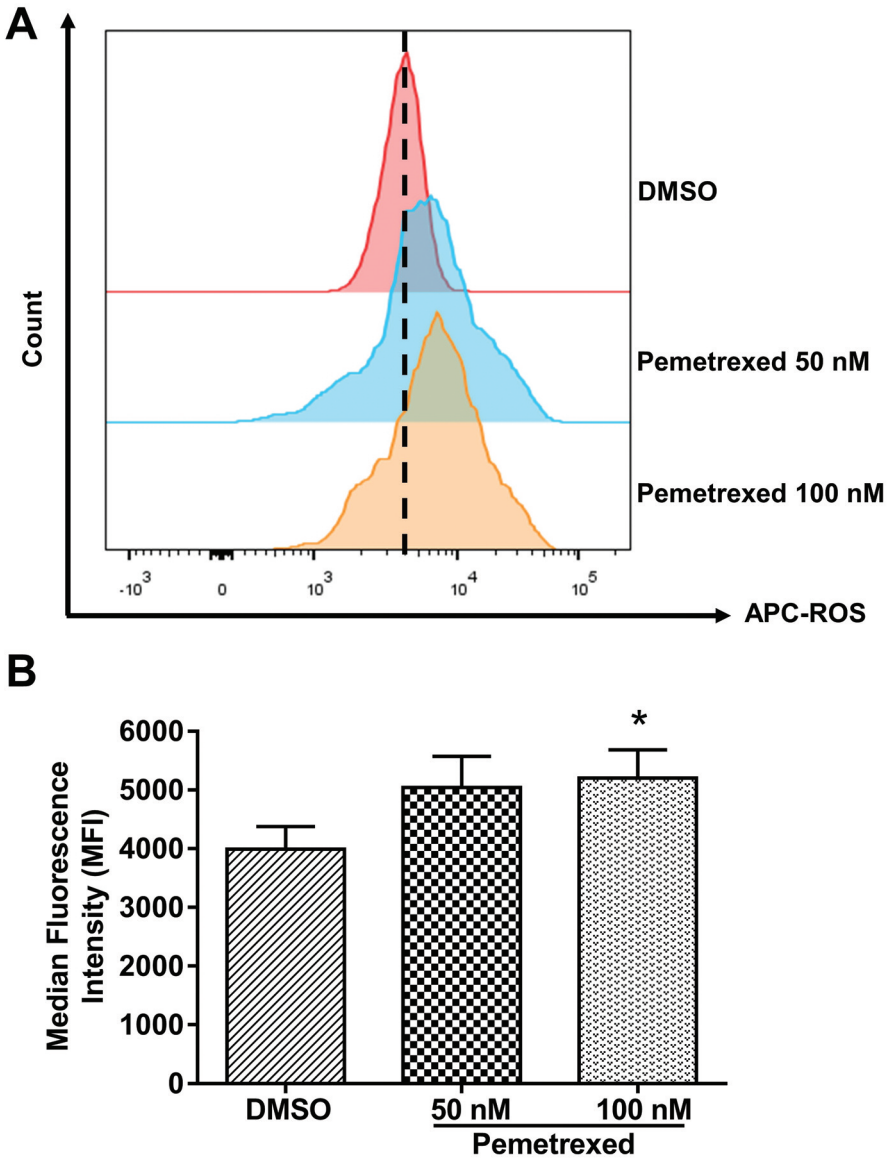

Figure 2. *Impact of pemetrexed on ROS generation. (A) FCM assessed the intracellular ROS levels in PC9 cells treated with different concentrations of pemetrexed. The signal was expressed in terms of the median fluorescence intensity (MFI). The histogram shows that ROS levels increased in a concentration-dependent manner. (B) The bar diagram shows that ROS production increased in a dose-dependent manner. The data (mean±SD) are illustrative of three technical replicates. Significance was determined by a one-way ANOVA followed by Dunnett's multiple comparison test: *p<0.05 compared to the DMSO-treated group.*

caspase-9, FasL, TRAIL, cleaved PARP, DR4, and FADD. The expression of Bax, tBid, cleaved caspase-3 (Asp 175), cleaved caspase-6 (Asp 162), cleaved caspase-7 (Asp 198), cleaved caspase-8, cleaved caspase-9, cleaved PARP, Fas, FasL, TRAIL, DR4, and FADD was significantly increased following pemetrexed treatment, whereas the Bcl-2 expression was significantly decreased (Figure 5C).

Western blotting was performed to evaluate the expression of cytochrome *c* of individual cytosolic and mitochondrial fractions in pemetrexed-treated PC9 cells. The results showed that the mitochondrial cytochrome *c* (mito cyt *c*) expression was significantly reduced, while the expression of cytosolic cytochrome *c* (cyto cyt *c*) was increased considerably. Furthermore, treatment with pemetrexed increased the Apaf-1 expression in the cytosol (cyto) of PC9 cells (Figure 5C).

Pemetrexed promoted cell-cycle arrest and senescence in PC9 cells. To determine whether or not pemetrexed induced

cell-cycle arrest, PC9 cells were treated with different concentrations of pemetrexed for 72 h and then subjected to FCM after DNA staining. As shown (Figure 6A, 6B), treatment with pemetrexed resulted in G_1 phase block in 95.07% of the population. The results indicate that pemetrexed caused cell-cycle arrest in G_1 phase.

Treatment with pemetrexed significantly decreased the levels of cyclin D1 and Cdk4 and increased the levels of mature-TGF-β (dimer), p-Smad2/3, and $p15^{INK4B}$. These results suggest that TGF-β inhibits Cyclin D1-Cdk4 complex activation through Smad2/Smad3 phosphorylation and the activation of $p15^{INK4B}$ (Figure 6C).

Cellular senescence is depicted as an irreversible arrest in the G_1 phase of the cell-cycle (32, 33). It begins with the inactivation of cyclin D1-Cdk4/6 complexes, which decisively control the progression of G_1 phase (34). We therefore analyzed the inductive impact of pemetrexed on the activity of SA-β-gal. We found that, with a relatively high dose (100 nM) of pemetrexed, the number of SA-β-gal-positive cells (senescent signals shown in green, indicated by red arrows) was greater and staining more potent than following treatment with 50 nM of pemetrexed (Figure 7).

Discussion

Pemetrexed is a known anticancer drug. However, the mechanism underlying its effects on PC9 cell death remains unclear. We, therefore, evaluated the extent of PC9 cell apoptosis mediated by pemetrexed.

In the intrinsic pathway of apoptosis, anti-apoptotic proteins (such as Bcl-2 and Bcl-xL) and proapoptotic proteins (such as Bim, Bik, Bid, Bak, Bax, Bad, and Bok) are important upstream molecules that respond to apoptosis. In different types of cancers, a decreased Bax/Bcl-2 ratio is usually detected and is closely related to a poor prognosis and tumor recurrence (35, 36). These proteins mainly exist in and direct the function of the mitochondrial membrane. Mitochondria produce ROS, which control the degree of redox in a cell. To maintain homeostasis, a low concentration of ROS is involved in several signal transduction pathways. When an apoptotic signal occurs in a cell, ROS production significantly increases through the apoptosis-related protein response to stress (37).

ROS-mediated oxidative stress can destroy parts of cells that contain proteins and DNA (38). A cell's failure to repair DNA damage *via* proper repair mechanisms can cause cell death through double-stranded DNA breaks. ROS can induce cell death by initiating various DNA damage response pathways, such as ATM-Chk2 and ATR-Chk1 (39).

Recent research has shown that the mitochondrial p53 Ser 15 phosphorylation activates Bak and Bax (40). The phosphorylation of p53 at Ser 46 controls a cell's ability to initiate apoptosis (41). Activated caspase-9 induces other molecules (including caspase-3, caspase-6, and caspase-7) to start the caspase cascade, leading to apoptosis (42-45). Caspase-3 is the primary killer involved in apoptosis, being either partially or totally liable for the proteolytic cleavage of numerous fundamental proteins, including the nuclear enzyme PARP (46).

Excessive ROS production within mitochondria reduces the MMP, affecting mitochondrial permeability and enhancing the release of mito cyt *c* into the cytosol from mitochondria (37, 47). Cytochrome *c* joins with Apaf-1 to form an apoptosome and activates apoptosis initiating procaspase-9 (47). The onset of the caspase cascade fills an essential role in apoptosis (48). Caspase-3 activation in the final stage of the cascade triggers apoptosis through the cellular component's degradation.

Our results showed that the intracellular ROS levels in pemetrexed-treated PC9 cells were significantly increased in a dose-dependent manner (Figure 2). During pemetrexed treatment, Chk1 was phosphorylated at Ser 345 and activated in an ATR-dependent manner (Figure 3C). These results show that pemetrexed significantly up-regulated the Bax expression but down-regulated the expression of Bcl-2 with increasing pemetrexed concentrations, suggesting an increase in the Bax/Bcl-2 ratio in PC9 cells treated with pemetrexed (Figure 5C). However, the intracellular MMP showed a decreasing trend after treatment with different concentrations of pemetrexed (Figure 4). In addition, after the separation of mitochondrial and cytosolic proteins, we evaluated the expression of mito and cyto cyt c.

The outcomes indicated that pemetrexed treatment triggered the down-regulation of mito cyt *c* but the up-regulation of cyto cyt *c*. Pemetrexed was thus deemed capable of inducing the release of cytochrome *c* into the cytosol from mitochondria (Figure 5C). In addition, pemetrexed increased the expression of cleaved caspase-9 and cleaved caspase-3 in a dose-dependent manner (Figure 5C). These results indicated that pemetrexed induced mitochondrial-dependent apoptosis in PC9 cells by activating Bax (proapoptotic protein) and inhibiting Bcl-2 (anti-apoptotic protein). Therefore, pemetrexed increased the ROS production and reduced the MMP, resulting in the release of cytochrome *c* into the cytosol from the mitochondria and thereby triggering an apoptotic event through the activation of caspase-9 and caspase-3.

The main constituents of death-inducing signaling complex (DISC) are TNF receptor, DR4 [TRAILR1] and DR5 [TRAILR2] receptors, Fas and FADD receptors. The extrinsic apoptotic pathway can be induced by apoptotic signals activating caspase-8 (49). Activated caspase-8 can indirectly cleave Bid for tBid or directly cleave caspase-3 to enhance apoptotic signals downstream. Subsequently, tBid moves further towards the mitochondrial membranes and induces their permeabilization (49, 50).

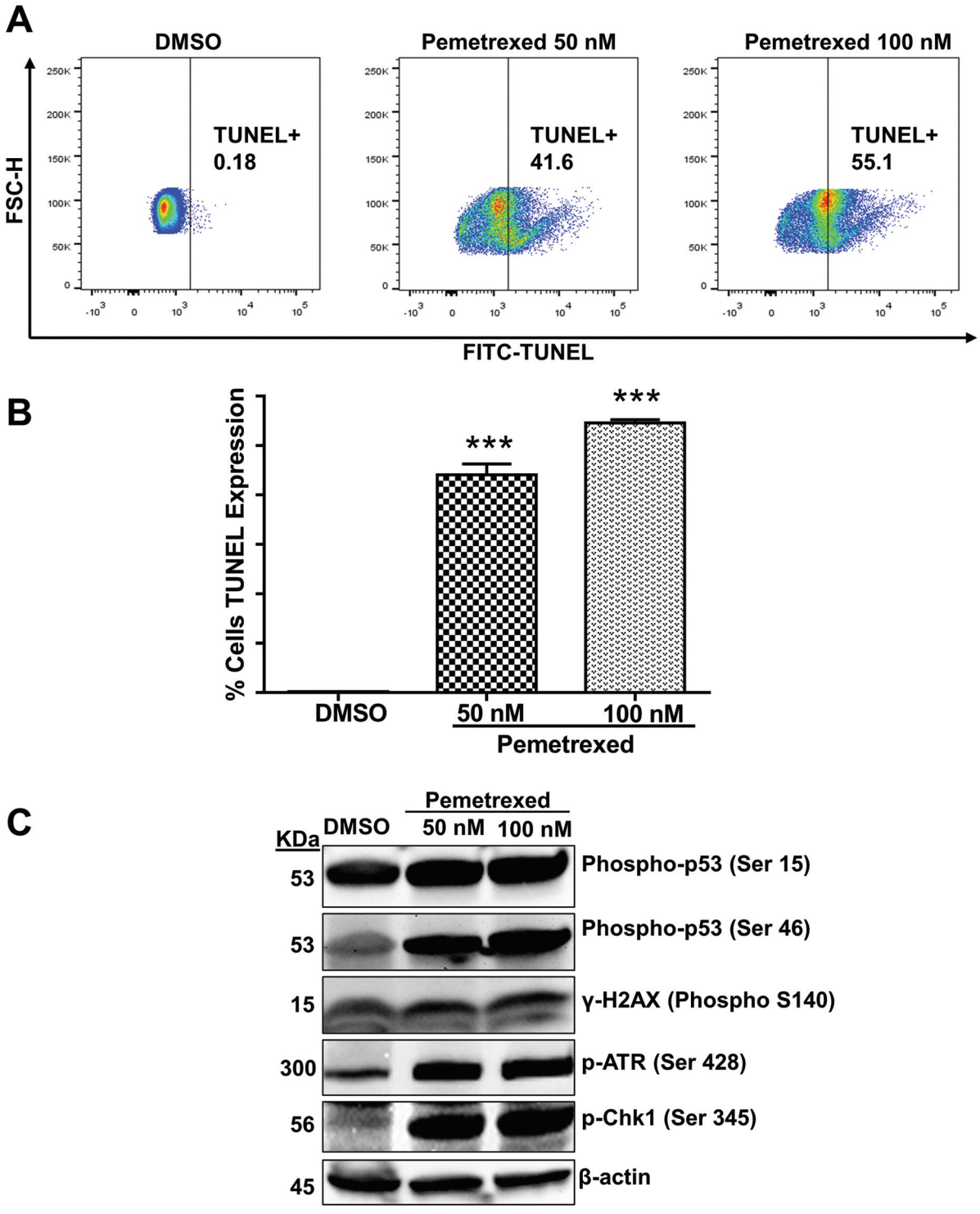

Figure 3. *Impact of pemetrexed on DNA fragmentation and the DNA damage signaling pathway. (A) PC9 cells were stained with fluorescein isothiocyanate-dUTP dye after incubation with pemetrexed at different concentrations for 72 h. The fluorescent signal was evaluated by flow cytometry. Dot plots show that DNA fragmentation increased in a concentration-dependent manner. (B) The bar graph represents the percentage of TUNEL-positive cells. Values are the mean±SD of three independent experiments. A one-way ANOVA followed by Dunnett's multiple comparison test confirmed the significance: ***p<0.001 compared to the DMSO group. (C) Western blotting shows the expression of p-ATR (Ser 428), p-Chk1 (Ser 345), phospho-p53 (Ser 15), phospho-p53 (Ser 46), and γ-H2AX (Phospho S140) in PC9 cells treated with pemetrexed after 72 h of exposure. β-actin served as an internal control. The immunoblots shown here are representative of three independent experiments.*

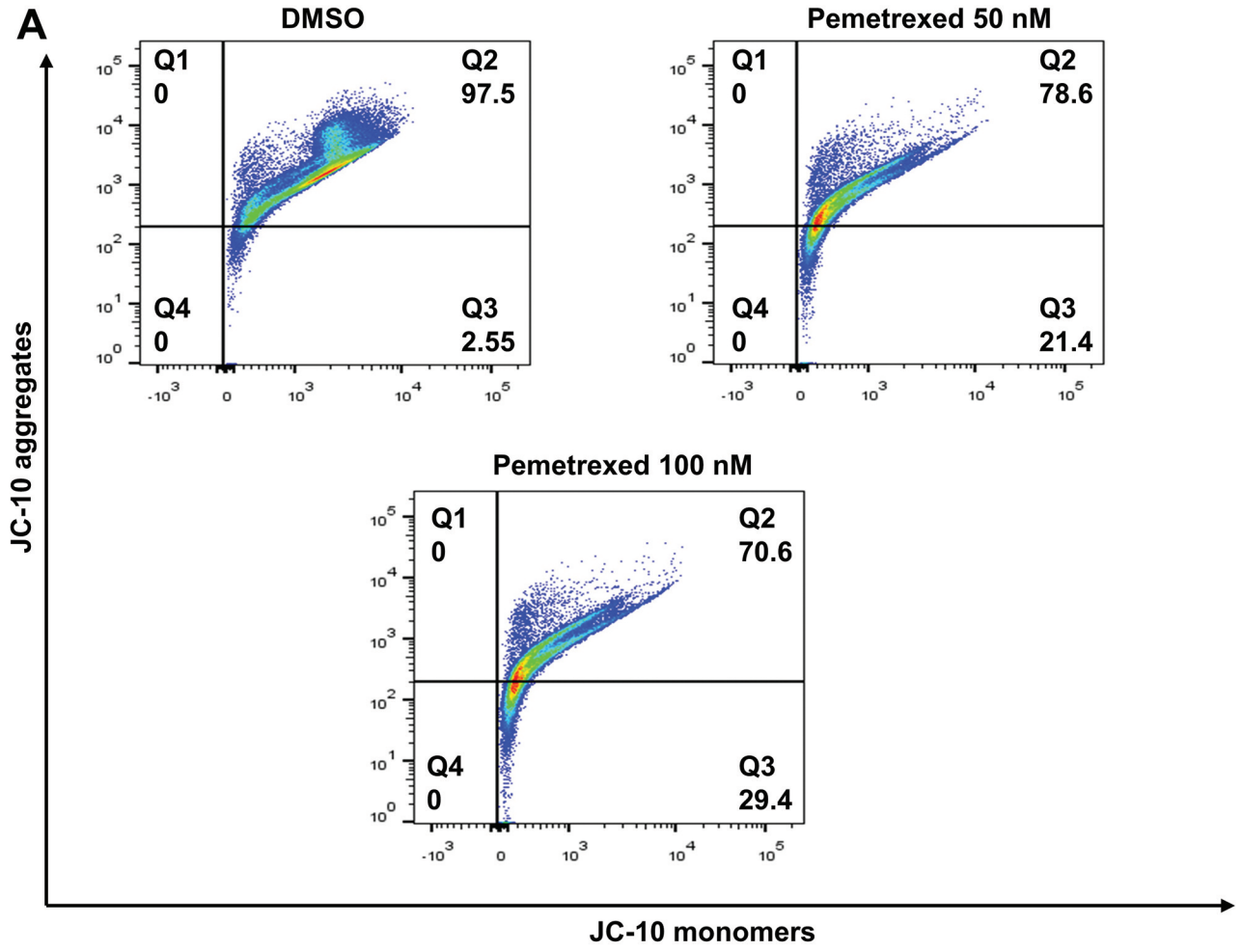

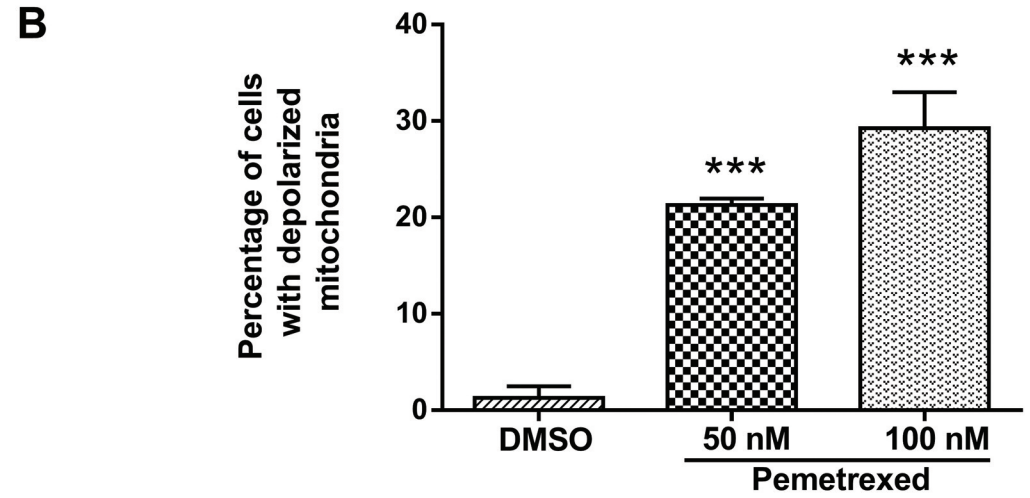

Figure 4. *Impact of pemetrexed on the mitochondrial membrane potential (MMP). (A) For 72 h, PC9 cells were treated with different concentrations of pemetrexed. Before the flow cytometry analysis, cells were stained with JC-10 dye. Representative results from three independent experiments. (B) Quantitative data are used from the green monomer fluorescence (depolarized MMP) of JC-10. Results are presented as the mean±SD of three independent measurements. Significance was determined by a one-way ANOVA followed by Dunnett's multiple comparison test: ***p<0.001 compared to the DMSO-treated group.*

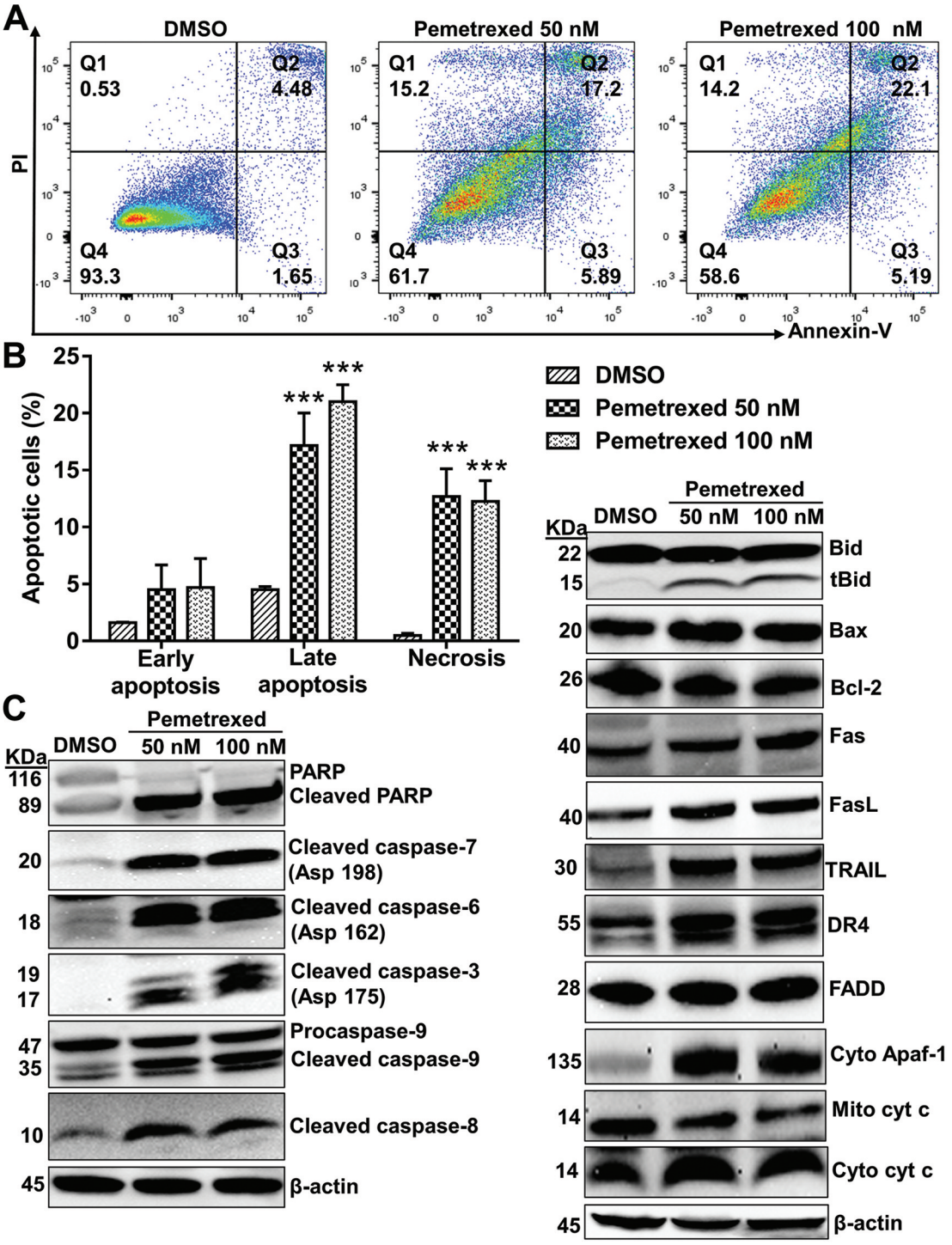

Figure 5. *Impact of pemetrexed on the induction of apoptosis in PC9 cells. (A) PC9 cells were treated with various pemetrexed concentrations, and flow cytometry (FCM) was used to evaluate apoptosis. Quadrant 1 shows necrotic cells; Quadrant 2 shows late-apoptotic cells; Quadrant 3 shows early apoptotic cells; Quadrant 4 shows viable cells. (B) The bar diagram represents the percent of apoptotic cells determined by FCM detection; n=3, Mean±SD; Significance was determined by a one-way ANOVA followed by Dunnett's multiple comparison test: ***p<0.001 compared with the DMSO (vehicle) group. (C) The expression of proteins related to the intrinsic and extrinsic pathways (Bax, Bcl-2, tBid, cleaved caspase-7 (Asp 198), cleaved caspase-6 (Asp 162), cleaved caspase-3 (Asp 175), cleaved caspase-9, cleaved caspase-8, cleaved PARP, Fas, FasL, TRAIL, DR4 and FADD) was detected by western blotting. The protein expression of cytosolic cytochrome c, Apaf-1, and mitochondrial cytochrome c was detected by Western blotting. β-actin was used as a loading control. The immunoblots shown here are representative of three independent experiments.*

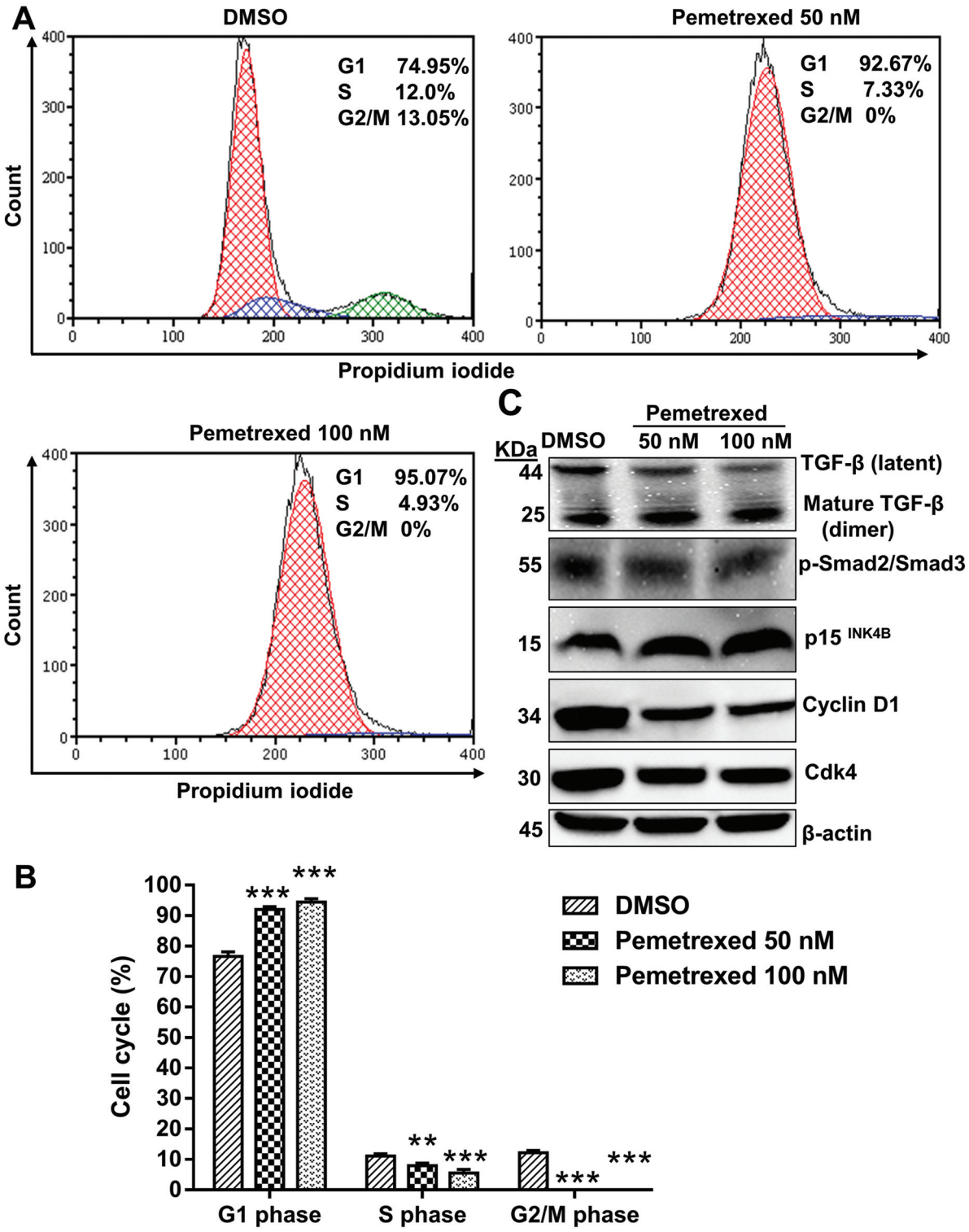

Figure 6. *Impact of pemetrexed on cell-cycle regulation in PC9 cells. (A) Flow cytometry showed that pemetrexed induced cell-cycle arrest in PC9 cells. (B) Cell-cycle distribution of PC9 cells. In the G_1 phase, the proportion of PC9 cells increased after 72 h of treatment with pemetrexed. Results are presented as the mean±SD of three independent experiments. Significance was determined by a one-way ANOVA followed by Dunnett's multiple comparison test: **p<0.01 and ***p<0.001 compared to the DMSO-treated group. (C) PC9 cells were treated with different concentrations of pemetrexed for 72 h. The cells were lysed, and the expression of TGF-β, p-Smad2/Smad3, $p15^{INK4B}$, Cyclin D1, and Cdk4 proteins was evaluated by Western blotting. β-actin was used as a loading control. The immunoblots shown here are representative of three independent experiments.*

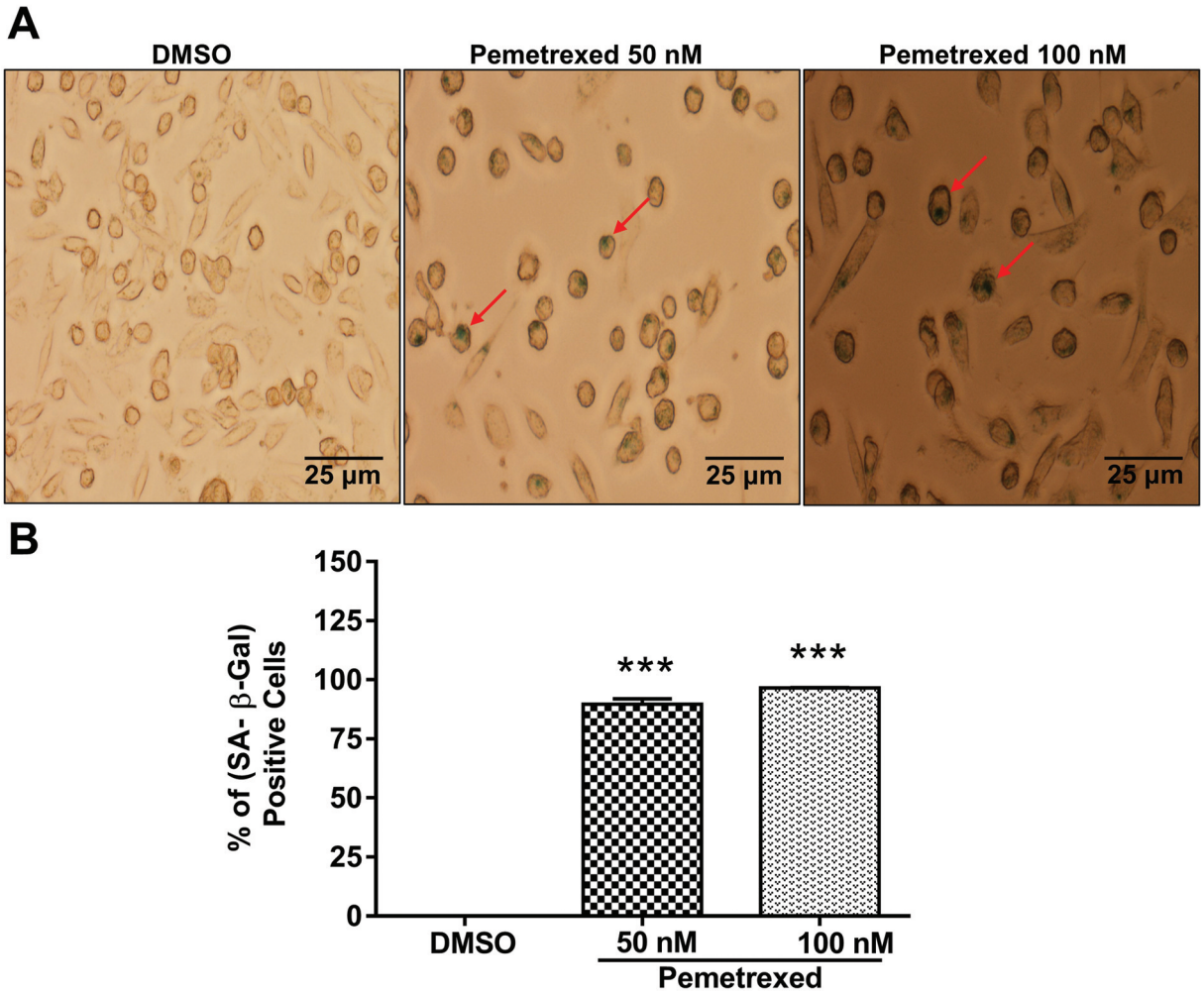

Figure 7. *Impact of pemetrexed on senescence induction in PC9 cells. (A) Before staining, PC9 cells were treated with different concentrations of pemetrexed with DMSO (control) for 72 h. Cells show SA-β-gal activity stained in green (red arrow). (B) Bar graphs represent the percentage of senescent cells. Results are presented as the mean±SD of three independent experiments. Significance was determined by a one-way ANOVA followed by Dunnett's multiple comparison test: ***p<0.001 compared to the DMSO group.*

We found that after the incubation of PC9 cells with pemetrexed at different concentrations, the expression of FasL, Fas, TRAIL, DR4, and cleaved caspase-8 was significantly increased (Figure 5C). This result indicated that pemetrexed activated the extrinsic apoptosis pathway through up-regulation of death receptors (Fas, DR4) and ligands (FasL, TRAIL) to induce the recruitment of adapter protein. This effect triggered caspase-8 activation resulted in PC9 cell apoptosis.

TGF-β is an effective cell proliferation inhibitor. In the G_1 phase, TGF-β induces growth arrest is mediated by Smad protein, which drives transcriptional targets, including c-myc (51-53). The inhibition of c-myc sensitizes cells to Cdk inhibitor (CKI) $p15^{INK4B}$, which represses Cdk4-Cyclin D (19, 54). In this study, we found that TGF-β-mediated G_1 phase arrest was triggered by p-Smad2/Smad3 proteins and inactivation of the Cyclin D1-Cdk4 complex (Figure 6C). TGF-β prompts senescence in various types of cancer cells (55-57). Our present findings showed that TGF-β mediated the accumulation of senescent PC9 cells during treatment with pemetrexed (Figure 7).

Conclusion

Pemetrexed repressed PC9 cell proliferation across three explicit systems (Figure 8). First, pemetrexed created ROS in PC9 cells, and ROS-mediated pressure caused cell death. Second, pemetrexed activated extrinsic and intrinsic

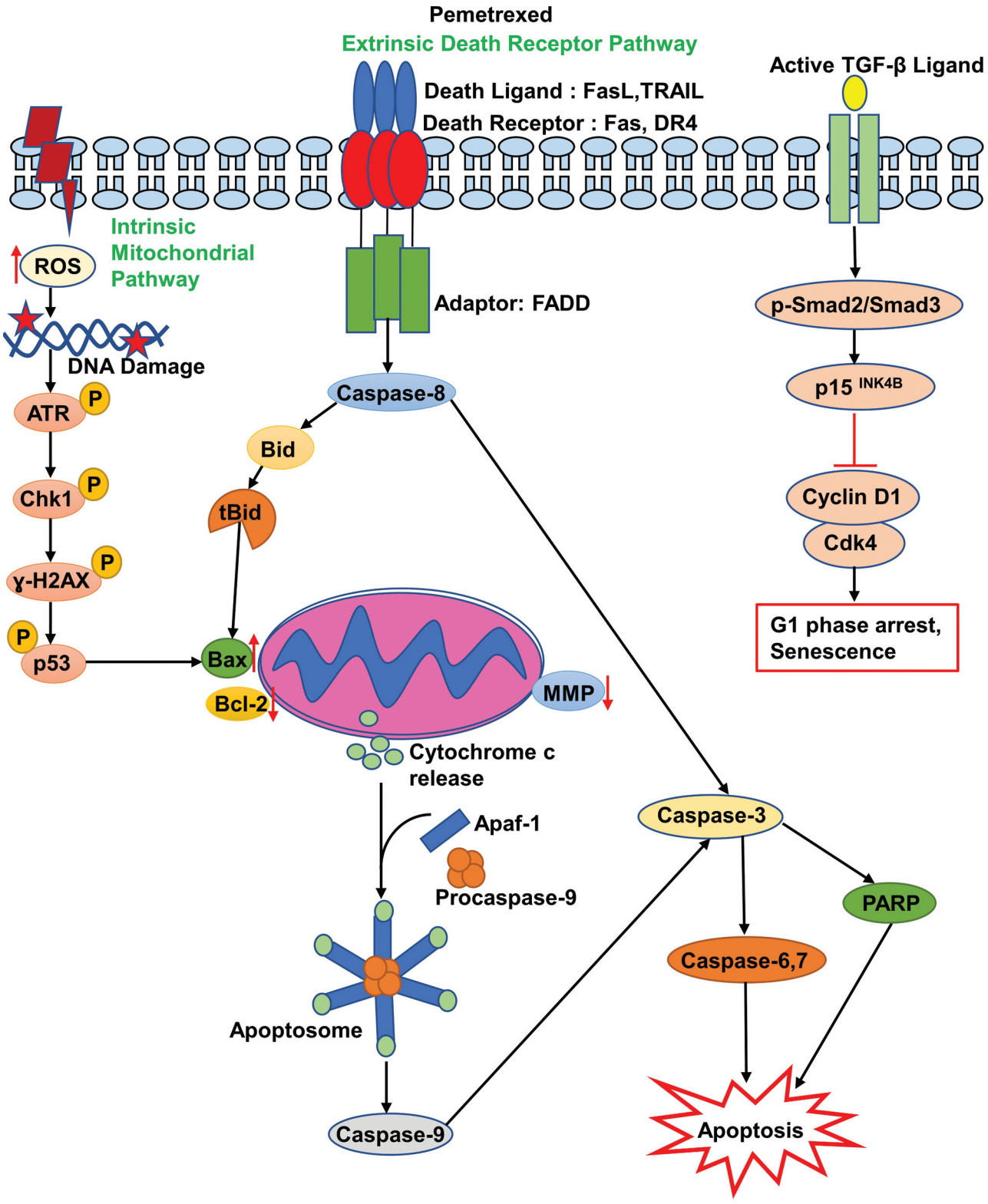

Figure 8. *Schematic diagram illustrating pemetrexed-induced G_1 arrest and apoptosis in PC9 cells.*

apoptotic signaling pathways *via* death receptors, cytochrome c, caspases, and proteolytic cleavage of PARP. Third, cell-cycle arrest was initiated by TGF-β-mediated G_1 arrest, which itself was induced by the inactivation of the Cyclin D1-Cdk4 complex. In these manner, pemetrexed showed a significant anticancer effect, and these findings strongly support an apoptotic capacity for pemetrexed.

Conflicts of Interest

The Authors declare no competing financial interests.

Authors' Contributions

Md Mohiuddin and Kazuo Kasahara conceived this study; Md Mohiuddin carried out the experiments; Md Mohiuddin and Kazuo Kasahara discussed and interpreted the results; Md Mohiuddin wrote the manuscript; Kazuo Kasahara supervised the experiments and project.

Acknowledgements

The Authors would like to thank Ms. Miki Kashiwano (Department of Respiratory Medicine, Graduate School of Medical Sciences, Kanazawa University) for her technical assistance. This work was supported by a Grant-in-Aid for Scientific Research (C) (JSPS KAKENHI Grant Number 17K09606) to K.K. The funders had no role in the study design, data collection or interpretation, or decision to submit the work for publication.

References

1 Siegel RL, Miller KD and Jemal A: Cancer statistics, 2018. CA Cancer J Clin *68(1)*: 7-30, 2018. PMID: 29313949. DOI: 10.3322/caac.21442

2 Hazarika M, White RM, Johnson JR and Pazdur R: FDA drug approval summaries: pemetrexed (Alimta). Oncologist *9(5)*: 482-488, 2004. PMID: 15477632. DOI: 10.1634/theoncologist.9-5-482

3 Felip E and Rosell R: Pemetrexed as second-line therapy for advanced non-small-cell lung cancer (NSCLC). Ther Clin Risk Manag *4(3)*: 579-585, 2008. PMID: 18827853. DOI: 10.2147/tcrm.s2248

4 Rafii S and Cullen MH: The role of maintenance pemetrexed in the treatment of non-small-cell lung cancer. Lung Cancer (Auckl) *1*: 101-106, 2010. PMID: 28210110. DOI: 10.2147/lctt.s11542

5 Pucci B, Kasten M and Giordano A: Cell cycle and apoptosis. Neoplasia *2(4)*: 291-299, 2000. PMID: 11005563. DOI: 10.1038/sj.neo.7900101

6 Hassan M, Watari H, AbuAlmaaty A, Ohba Y and Sakuragi N: Apoptosis and molecular targeting therapy in cancer. Biomed Res Int *2014*: 150845, 2014. PMID: 25013758. DOI: 10.1155/2014/150845

7 Schieber M and Chandel NS: ROS function in redox signaling and oxidative stress. Curr Biol *24(10)*: R453-R462, 2014. PMID: 24845678. DOI: 10.1016/j.cub.2014.03.034

8 Kao SJ, Lee WJ, Chang JH, Chow JM, Chung CL, Hung WY and Chien MH: Suppression of reactive oxygen species-mediated ERK and JNK activation sensitizes dihydromyricetin-induced mitochondrial apoptosis in human non-small cell lung cancer. Environ Toxicol *32(4)*: 1426-1438, 2017. PMID: 27539140. DOI: 10.1002/tox.22336

9 Srinivas US, Tan BWQ, Vellayappan BA and Jeyasekharan AD: ROS and the DNA damage response in cancer. Redox Biol *25*: 101084, 2019. PMID: 30612957. DOI: 10.1016/j.redox.2018.101084

10 Fan PC, Zhang Y, Wang Y, Wei W, Zhou YX, Xie Y, Wang X, Qi YZ, Chang L, Jia ZP, Zhou Z, Guan H, Zhang H, Xu P and Zhou PK: Quantitative proteomics reveals mitochondrial respiratory chain as a dominant target for carbon ion radiation: Delayed reactive oxygen species generation caused DNA damage. Free Radic Biol Med *130*: 436-445, 2019. PMID: 30395972. DOI: 10.1016/j.freeradbiomed.2018.10.449

11 Hockenbery DM, Oltvai ZN, Yin XM, Milliman CL and Korsmeyer SJ: Bcl-2 functions in an antioxidant pathway to prevent apoptosis. Cell *75(2)*: 241-251, 1993. PMID: 7503812. DOI: 10.1016/0092-8674(93)80066-n

12 Kim R, Emi M and Tanabe K: Role of mitochondria as the gardens of cell death. Cancer Chemother Pharmacol *57(5)*: 545-553, 2006. PMID: 16175394. DOI: 10.1007/s00280-005-0111-7

13 Daniel PT, Wieder T, Sturm I and Schulze-Osthoff K: The kiss of death: promises and failures of death receptors and ligands in cancer therapy. Leukemia *15(7)*: 1022-1032, 2001. PMID: 11455969. DOI: 10.1038/sj.leu.2402169

14 Pozzesi N, Fierabracci A, Liberati AM, Martelli MP, Ayroldi E, Riccardi C and Delfino DV: Role of caspase-8 in thymus function. Cell Death Differ *21(2)*: 226-233, 2014. PMID: 24270406. DOI: 10.1038/cdd.2013.166

15 Li H, Zhu H, Xu CJ and Yuan J: Cleavage of BID by caspase 8 mediates the mitochondrial damage in the Fas pathway of apoptosis. Cell *94(4)*: 491-501, 1998. PMID: 9727492. DOI: 10.1016/s0092-8674(00)81590-1

16 Kim HE, Du F, Fang M and Wang X: Formation of apoptosome is initiated by cytochrome c-induced dATP hydrolysis and subsequent nucleotide exchange on Apaf-1. Proc Natl Acad Sci USA *102(49)*: 17545-17550, 2005. PMID: 16251271. DOI: 10.1073/pnas.0507900102

17 Malanga M and Althaus FR: The role of poly(ADP-ribose) in the DNA damage signaling network. Biochem Cell Biol *83(3)*: 354-364, 2005. PMID: 15959561. DOI: 10.1139/o05-038

18 Meikrantz W and Schlegel R: Apoptosis and the cell cycle. J Cell Biochem *58(2)*: 160-174, 1995. PMID: 7673324. DOI: 10.1002/jcb.240580205

19 Hannon GJ and Beach D: p15INK4B is a potential effector of TGF-beta-induced cell cycle arrest. Nature *371(6494)*: 257-261, 1994. PMID: 8078588. DOI: 10.1038/371257a0

20 Iavarone A and Massagué J: Repression of the CDK activator Cdc25A and cell-cycle arrest by cytokine TGF-beta in cells lacking the CDK inhibitor p15. Nature *387(6631)*: 417-422, 1997. PMID: 9163429. DOI: 10.1038/387417a0

21 Ewen ME, Sluss HK, Whitehouse LL and Livingston DM: TGF beta inhibition of Cdk4 synthesis is linked to cell cycle arrest. Cell *74(6)*: 1009-1020, 1993. PMID: 8402878. DOI: 10.1016/0092-8674(93)90723-4

22 Zhang H, Feng QQ, Gong JH and Ma JP: Anticancer effects of isofraxidin against A549 human lung cancer cells *via* the EGFR signaling pathway. Mol Med Rep *18(1)*: 407-414, 2018. PMID: 29750303. DOI: 10.3892/mmr.2018.8950

23 Wainwright LJ, Lasorella A and Iavarone A: Distinct mechanisms of cell cycle arrest control the decision between differentiation and senescence in human neuroblastoma cells. Proc Natl Acad Sci USA *98(16)*: 9396-9400, 2001. PMID: 11481496. DOI: 10.1073/pnas.161288698

24 Mansilla S, Piña B and Portugal J: Daunorubicin-induced variations in gene transcription: commitment to proliferation arrest, senescence and apoptosis. Biochem J *372(Pt 3)*: 703-711, 2003. PMID: 12656675. DOI: 10.1042/BJ20021950

25 Han Z, Wei W, Dunaway S, Darnowski JW, Calabresi P, Sedivy J, Hendrickson EA, Balan KV, Pantazis P and Wyche JH: Role of p21 in apoptosis and senescence of human colon cancer cells treated with camptothecin. J Biol Chem *277(19)*: 17154-17160, 2002. PMID: 11877436. DOI: 10.1074/jbc.M112401200

26 Sakai A, Kasahara K, Ohmori T, Kimura H, Sone T, Fujimura M and Nakao S: MET increases the sensitivity of gefitinib-resistant cells to SN-38, an active metabolite of irinotecan, by up-regulating the topoisomerase I activity. J Thorac Oncol *7(9)*: 1337-1344, 2012. PMID: 22722827. DOI: 10.1097/JTO.0b013e31825cca4c

27 Abraham RT: Cell cycle checkpoint signaling through the ATM and ATR kinases. Genes Dev *15(17)*: 2177-2196, 2001. PMID: 11544175. DOI: 10.1101/gad.914401

28 Turner T and Caspari T: When heat casts a spell on the DNA damage checkpoints. Open Biol *4*: 140008, 2014. PMID: 24621867. DOI: 10.1098/rsob.140008

29 Boohaker RJ and Xu B: The versatile functions of ATM kinase. Biomed J *37(1)*: 3-9, 2014. PMID: 24667671. DOI: 10.4103/2319-4170.125655

30 Guo C, Sun L, Chen X and Zhang D: Oxidative stress, mitochondrial damage and neurodegenerative diseases. Neural Regen Res *8(21)*: 2003-2014, 2013. PMID: 25206509. DOI: 10.3969/j.issn.1673-5374.2013.21.009

31 Li S, Dong P, Wang J, Zhang J, Gu J, Wu X, Wu W, Fei X, Zhang Z, Wang Y, Quan Z and Liu Y: Icariin, a natural flavonol glycoside, induces apoptosis in human hepatoma SMMC-7721 cells *via* a ROS/JNK-dependent mitochondrial pathway. Cancer Lett *298(2)*: 222-230, 2010. PMID: 20674153. DOI: 10.1016/j.canlet.2010.07.009

32 Stein GH and Dulić V: Origins of G1 arrest in senescent human fibroblasts. Bioessays *17(6)*: 537-543, 1995. PMID: 7575495. DOI: 10.1002/bies.950170610

33 Smith JR and Pereira-Smith OM: Replicative senescence: implications for *in vivo* aging and tumor suppression. Science *273(5271)*: 63-67, 1996. PMID: 8658197. DOI: 10.1126/science.273.5271.63

34 Dulić V, Drullinger LF, Lees E, Reed SI and Stein GH: Altered regulation of G1 cyclins in senescent human diploid fibroblasts: accumulation of inactive cyclin E-Cdk2 and cyclin D1-Cdk2 complexes. Proc Natl Acad Sci USA *90(23)*: 11034-11038, 1993. PMID: 8248208. DOI: 10.1073/pnas.90.23.11034

35 Prokop A, Wieder T, Sturm I, Essmann F, Seeger K, Wuchter C, Ludwig WD, Henze G, Dörken B and Daniel PT: Relapse in childhood acute lymphoblastic leukemia is associated with a decrease of the Bax/Bcl-2 ratio and loss of spontaneous caspase-3 processing *in vivo*. Leukemia *14(9)*: 1606-1613, 2000. PMID: 10995007. DOI: 10.1038/sj.leu.2401866

36 Raisova M, Hossini AM, Eberle J, Riebeling C, Wieder T, Sturm I, Daniel PT, Orfanos CE and Geilen CC: The Bax/Bcl-2 ratio determines the susceptibility of human melanoma cells to CD95/Fas-mediated apoptosis. J Invest Dermatol *117(2)*: 333-340, 2001. PMID: 11511312. DOI: 10.1046/j.0022-202x.2001.01409.x

37 Fulda S, Galluzzi L and Kroemer G: Targeting mitochondria for cancer therapy. Nat Rev Drug Discov *9(6)*: 447-464, 2010. PMID: 20467424. DOI: 10.1038/nrd3137

38 Helleday T, Petermann E, Lundin C, Hodgson B and Sharma RA: DNA repair pathways as targets for cancer therapy. Nat Rev Cancer *8(3)*: 193-204, 2008. PMID: 18256616. DOI: 10.1038/nrc2342

39 Sahu RP, Batra S and Srivastava SK: Activation of ATM/Chk1 by curcumin causes cell cycle arrest and apoptosis in human pancreatic cancer cells. Br J Cancer *100(9)*: 1425-1433, 2009. PMID: 19401701. DOI: 10.1038/sj.bjc.6605039

40 Nieminen AI, Eskelinen VM, Haikala HM, Tervonen TA, Yan Y, Partanen JI and Klefström J: Myc-induced AMPK-phospho p53 pathway activates Bak to sensitize mitochondrial apoptosis. Proc Natl Acad Sci USA *110(20)*: E1839-E1848, 2013. PMID: 23589839. DOI: 10.1073/pnas.1208530110

41 Oda K, Arakawa H, Tanaka T, Matsuda K, Tanikawa C, Mori T, Nishimori H, Tamai K, Tokino T, Nakamura Y and Taya Y: p53AIP1, a potential mediator of p53-dependent apoptosis, and its regulation by Ser-46-phosphorylated p53. Cell *102(6)*: 849-862, 2000. PMID: 11030628. DOI: 10.1016/s0092-8674(00)00073-8

42 Deveraux QL, Roy N, Stennicke HR, Van Arsdale T, Zhou Q, Srinivasula SM, Alnemri ES, Salvesen GS and Reed JC: IAPs block apoptotic events induced by caspase-8 and cytochrome *c* by direct inhibition of distinct caspases. EMBO J *17(8)*: 2215-2223, 1998. PMID: 9545235. DOI: 10.1093/emboj/17.8.2215

43 Slee EA, Harte MT, Kluck RM, Wolf BB, Casiano CA, Newmeyer DD, Wang HG, Reed JC, Nicholson DW, Alnemri ES, Green DR and Martin SJ: Ordering the cytochrome c-initiated caspase cascade: hierarchical activation of caspases-2, -3, -6, -7, -8, and -10 in a caspase-9-dependent manner. J Cell Biol *144(2)*: 281-292, 1999. PMID: 9922454. DOI: 10.1083/jcb.144.2.281

44 Sun XM, MacFarlane M, Zhuang J, Wolf BB, Green DR and Cohen GM: Distinct caspase cascades are initiated in receptor-mediated and chemical-induced apoptosis. J Biol Chem *274(8)*: 5053-5060, 1999. PMID: 9988752. DOI: 10.1074/jbc.274.8.5053

45 MacFarlane M, Cain K, Sun XM, Alnemri ES and Cohen GM: Processing/activation of at least four interleukin-1beta converting enzyme-like proteases occurs during the execution phase of apoptosis in human monocytic tumor cells. J Cell Biol *137(2)*: 469-479, 1997. PMID: 9128256. DOI: 10.1083/jcb.137.2.469

46 Fernandes-Alnemri T, Litwack G and Alnemri ES: CPP32, a novel human apoptotic protein with homology to Caenorhabditis elegans cell death protein Ced-3 and mammalian interleukin-1 beta-converting enzyme. J Biol Chem *269(49)*: 30761-30764, 1994. PMID: 7983002.

47 Kroemer G, Galluzzi L and Brenner C: Mitochondrial membrane permeabilization in cell death. Physiol Rev *87(1)*: 99-163, 2007. PMID: 17237344. DOI: 10.1152/physrev.00013.2006

48 Galluzzi L, López-Soto A, Kumar S and Kroemer G: Caspases connect cell-death signaling to organismal homeostasis. Immunity *44(2)*: 221-231, 2016. PMID: 26885855. DOI: 10.1016/j.immuni.2016.01.020

49 Ashkenazi A: Targeting the extrinsic apoptosis pathway in cancer. Cytokine Growth Factor Rev *19(3-4)*: 325-331, 2008. PMID: 18495520. DOI: 10.1016/j.cytogfr.2008.04.001

50 Adams JM and Cory S: The Bcl-2 apoptotic switch in cancer development and therapy. Oncogene *26(9)*: 1324-1337, 2007. PMID: 17322918. DOI: 10.1038/sj.onc.1210220

51 Chen CR, Kang Y, Siegel PM and Massagué J: E2F4/5 and p107 as Smad cofactors linking the TGFbeta receptor to c-myc repression. Cell *110(1)*: 19-32, 2002. PMID: 12150994. DOI: 10.1016/s0092-8674(02)00801-2

52 Coffey RJ Jr, Bascom CC, Sipes NJ, Graves-Deal R, Weissman BE and Moses HL: Selective inhibition of growth-related gene expression in murine keratinocytes by transforming growth factor beta. Mol Cell Biol *8(8)*: 3088-3093, 1988. PMID: 2463471. DOI: 10.1128/mcb.8.8.3088

53 Pietenpol JA, Holt JT, Stein RW and Moses HL: Transforming growth factor beta 1 suppression of c-myc gene transcription: role in inhibition of keratinocyte proliferation. Proc Natl Acad Sci USA *87(10)*: 3758-3762, 1990. PMID: 2187192. DOI: 10.1073/pnas.87.10.3758

54 Warner BJ, Blain SW, Seoane J and Massagué J: Myc downregulation by transforming growth factor beta required for activation of the p15(Ink4b) G(1) arrest pathway. Mol Cell Biol *19(9)*: 5913-5922, 1999. PMID: 10454538. DOI: 10.1128/mcb.19.9.5913

55 Debacq-Chainiaux F, Borlon C, Pascal T, Royer V, Eliaers F, Ninane N, Carrard G, Friguet B, de Longueville F, Boffe S, Remacle J and Toussaint O: Repeated exposure of human skin fibroblasts to UVB at subcytotoxic level triggers premature senescence through the TGF-beta1 signaling pathway. J Cell Sci *118(Pt 4)*: 743-758, 2005. PMID: 15671065. DOI: 10.1242/jcs.01651

56 Minagawa S, Araya J, Numata T, Nojiri S, Hara H, Yumino Y, Kawaishi M, Odaka M, Morikawa T, Nishimura SL, Nakayama K and Kuwano K: Accelerated epithelial cell senescence in IPF and the inhibitory role of SIRT6 in TGF-β-induced senescence of human bronchial epithelial cells. Am J Physiol Lung Cell Mol Physiol *300(3)*: L391-L401, 2011. PMID: 21224216. DOI: 10.1152/ajplung.00097.2010

57 Senturk S, Mumcuoglu M, Gursoy-Yuzugullu O, Cingoz B, Akcali KC and Ozturk M: Transforming growth factor-beta induces senescence in hepatocellular carcinoma cells and inhibits tumor growth. Hepatology *52(3)*: 966-974, 2010. PMID: 20583212. DOI: 10.1002/hep.23769

Received April 5, 2021
Revised April 27, 2021
Accepted May 6, 2021